

Ground- and excited-state reactivity of some ketenylcarbenes

D. Dogaru,¹ N. Pietri,² J. P. Aycard² and M. Hillebrand^{1*}

¹Department of Physical Chemistry, University of Bucharest, Bdul. Regina Elisabeta 4–12, RO-7034 Bucharest, Romania

²UMR CNRS 6633, Physique des Interactions Ioniques et Moléculaires, Equipe Spectrométries et Dynamique Moléculaire, Université de Provence, Case 252, Centre de St. Jérôme, 13397 Marseille Cedex 20, France

Received 14 October 2003; revised 4 December 2003; accepted 12 December 2003

epoc

ABSTRACT: The reactivity of ketenylcarbenes has been widely discussed on experimental and theoretical grounds in connection with the photochemical decomposition in cryogenic matrices of some substituted cyclobutenediones and maleic anhydrides. It was found that, although the presence of these intermediates was postulated in the decomposition mechanisms, only monofluoroketenylcarbene was experimentally evidenced and characterized by its IR spectrum. In all other cases, the experimental data revealed the formation of the corresponding cyclopropenones and, under continuing irradiation, of the alkynes. Theoretical calculations also point to their high reactivity towards the ring closure reaction. In order to gain an insight into the main factors determining the ketenylcarbene reactivity, *ab initio* calculations on both the ground (HF/6–31G* and MP2/6–31G*) and the first excited state (HF/6–31G*) were performed. The results indicate that the ring closure reaction is mainly determined by the electrostatic interaction between the carbene center and the C α atom of the ketenyl group. The role of the in-plane interaction between the molecular orbital localized on the carbene center and the first two vacant orbitals is also discussed. The excited-state optimized geometries allow for the characterization of the excited-state reactivity. Copyright © 2004 John Wiley & Sons, Ltd.

Additional material for this paper is available in Wiley InterScience

KEYWORDS: ketenylcarbenes; cyclopropenones; HF-6–31G* calculations; ground state geometries; excited state geometries

INTRODUCTION

The reaction mechanism suggested for the photochemical decomposition of mono- and dicarbonyl compounds isolated in rare gas cryogenic matrices assumes the formation of highly reactive intermediates, carbenes, which undergo further subsequent reactions towards the final products.^{1–10}

In the cases of some conjugated carbenes, allenyl³ and substituted ketenylcarbenes, the main reactions leading to the final stable compounds were ring closure, hydrogen or chlorine migration and/or CO elimination.

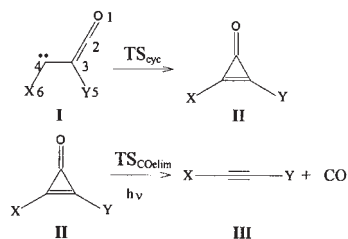
Our previous studies showed that starting either from dichlorocyclobutenedione⁴ or from maleic and dichloromaleic anhydrides,⁵ similar final products were isolated, i.e. cyclopropenones or, with time and under continuous irradiation, the corresponding alkynes. In the case of dichlorocyclobutenedione, in addition to dichlorocyclopropenone, small amounts of dichloropropadienone were

also identified, but a kinetic survey of the respective formation rate constants reveals a ratio of 13:1. On further irradiation, the single product was dichloroacetylene. A similar behavior was reported starting with other substituted cyclobutenediones⁷ or maleic anhydrides^{8,9} and was carefully analyzed by Sung *et al.*¹⁰ In the suggested mechanisms, the presence as an intermediate of the *syn*-ketenylcarbene was assumed (see Scheme 1).

In spite of various experimental studies devoted to ketenylcarbenes, a survey of literature data shows that only in a single case was a ketenylcarbene identified and characterized by its IR spectrum, namely the fluoroketenylcarbene obtained by Dailey⁹ in the photolysis of fluoromaleic anhydride.

Supporting the experimental data, the theoretical calculations predict a low activation energy for the ring closure reaction. For the unsubstituted and dichlorosubstituted ketenylcarbenes at the HF level, we previously obtained 2.4 and 3.1 kcal mol^{–1}, respectively, and for the fluoroketenylcarbene Dailey⁹ found 2.7 kcal mol^{–1} (1 kcal = 4.18 kJ). At the MP2 level, Sung *et al.*¹⁰ reported that for some symmetrically disubstituted ketenylcarbenes it was not possible to locate a transition state for the ring closure. They stated that

*Correspondence to: M. Hillebrand, Department of Physical Chemistry, University of Bucharest, Bdul. Regina Elisabeta 4–12, RO-7034 Bucharest, Romania. E-Mail: mihh@gw-chimie.math.unibuc.ro
Contract/grant sponsor: CNCSIS-Romania; Contract/grant number: 33618/2002.



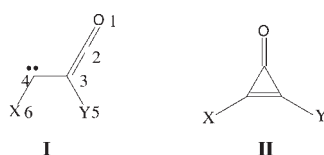
Scheme 1

cyclopropenones are formed by a concerted reaction with the decarbonylation reaction of bisketenes leading to the ketenylcarbenes. Our previous MP2 calculations on the dichloroketenylcarbene led to the same result, only the dichlorocyclopropenone minimum being located.^{5,6}

Considering the experimental data, this study started from two facts, the high reactivity of the ketenylcarbenes, which prevents their experimental identification, and the special case of the fluoroketenylcarbene. From the theoretical point of view, the failure to locate for some ketenylcarbenes, at the MP2 level, a carbene structure makes us presume that the introduction of electronic correlation enhances those electronic features which are mostly correlated with the reactivity in the ring closure reaction.

The aims of this work were twofold: an analysis of the electronic factors that determine the reactivity of the ketenylcarbenes and the characterization of the excited-state properties for both the ketenylcarbenes (**I**) and the corresponding cyclopropenones (**II**), in order to explain the effect of the irradiation time on the system evolution.

The investigated compounds are presented in Fig. 1 and can be classified in three series according to the substituted positions. Series **a** represents the compounds substituted at the carbene center and series **b** those



a	Y=H	b	X=H	c	X=Y
1:	X = H; (HF)				
2a:	X = F; (HF, MP2)	2b:	Y = F; (HF)	2c:	X = Y = F; (HF)
3a:	X = Cl; (HF, MP2)	3b:	Y = Cl; (HF)	3c:	X = Y = Cl; (HF)
4a:	X = OH; (HF, MP2)	4b:	Y = OH; (HF)	4c:	X = Y = OH; (HF, MP2)
5a:	X = NH ₂ ; (HF, MP2)	5b:	Y = NH ₂ ; (HF)	5c:	X = Y = NH ₂ ; (HF, MP2)
6a:	X = CN; (HF)	6b:	Y = CN; (HF)	6c:	X = Y = CN; (HF)
7a:	X = CH ₃ ; (HF)	7b:	Y = CH ₃ ; (HF)	7c:	X = Y = CH ₃ ; (HF)

Figure 1. The investigated compounds and the numbering of the atoms. For the ketenylcarbenes the first label is **I** and for the corresponding cyclopropenones **II**. The entries in parentheses indicate the level of calculation, HF/6-31G**/HF/6-31G* (HF) or MP2/6-31G**/MP2/6-31G* (MP2) at which stable ketenylcarbene open forms were located. For the ketenylcarbene **I-4b** the corresponding cyclopropenone was obtained even at the HF/6-31G* level

substituted at the ketenyl moiety. The compounds in series **c** are symmetrically substituted at both positions. The reactions considered are those presented in Scheme 1, the ring closure reaction and the CO elimination.

Two sources can be assumed for the presence of the alkyne in the system: CO elimination from either the *syn*-ketenylcarbenes or cyclopropenones and CO elimination from the *anti*-ketenylcarbenes, formed at the same time as the *syn*-carbenes in the first step of irradiation of the carbonyl compounds.⁹ Since the experimental data show that the alkyne accumulation occurs at long irradiation time and mainly after the total disappearance of the corresponding cyclopropenone from the system, we shall focus on the first possibility.

One of the most discussed aspects of the electronic structure of carbenes is the singlet or triplet nature of the ground state. As long as the ring closure and the CO elimination reactions are considered, it is more likely that the singlet state is implied. We have shown⁵ that the triplet state could be responsible for the 1,2 shift reactions starting from the *anti*-ketenylcarbenes and leading to propadienones. Accordingly, the following discussion will be focused on the electronic features of the singlet state.

The following points will be developed: (i) the possibility of nucleophilic attack of the carbene lone pair on the ketene C α atom as the cause of the facile ring closure reaction and the role of the electrostatic interaction between the carbon atoms directly implied in the formation of the new bond, C2 and C4; this implies a survey of the ground state (S_0) frontier molecular orbitals calculated at HF and MP2 levels in order to identify the electronic features mostly influenced by the introduction of the electronic correlation; (ii) the discussion of the optimized geometry and the relative energies of the first excited singlet states (S_1). One can consider that the main geometric parameters of the excited transition states for the ring closure and decarbonylation reactions are not modified to a great extent in comparison with those of the ground state. Therefore, the comparison of the S_1 geometry for both carbenes and cyclopropenones with the geometry of the ground transition states corresponding to these reactions will reveal the tendency in the excited-state reactivity.

COMPUTATIONAL DETAILS

Ab initio, HF/6-31G**/HF/6-31G* and MP2/6-31G**/MP2/6-31G*, calculations were performed for the singlet and triplet states (ROHF) of the ketenylcarbenes in Fig. 1 using the GAMESS program.¹¹ The *syn-z* geometries implied in the cyclization process were considered. The optimizations of the excited states were performed using the TRUDGE non-gradient optimizer implemented in the same program, followed by CISD calculations. The active space was limited to the last four occupied and first four vacant orbitals.

In order to check the method for the excited states, the ground-state geometry was also optimized by the same technique and the results were compared with those obtained by gradients methods. The saddle points localized on the ground-state surface were checked by the Hessian matrix. For the sake of comparison with excited-state results, single-point CI calculations implying the same configurations as for the excited state optimizations were performed at the geometry of the saddle points.

RESULTS AND DISCUSSION

Ground-state electronic structure

In order to establish the nature of the ground state, all the singlet and triplet carbene states were optimized under the same conditions at both the HF and MP2 levels. In addition, the transition states corresponding to the two reactions considered, TS_{cyc} and $\text{TS}_{\text{CO elim}}$, were located.

The singlet–triplet gaps, ΔE_{ST} , are listed in Table 1. The data show that the HF (singlet states) and ROHF (triplet states) calculations predict for all the investigated ketenylcarbenes a singlet ground state. A special mention must be made for the unsubstituted ketenylcarbene **I-1**. Differing from the previous UHF calculations, the ground state is a singlet, but the singlet–triplet gap is very small.

For the other compounds, the large ΔE_{ST} values, especially for series **a** and **c**, show that the ground singlet state and the triplet are well separated. In the case of the fluoro-substituted ketenylcarbenes, this result is in agreement with the statement that fluorine directly attached to a carbene carbon strongly favors the singlet state.¹² The optimized geometries reflect the difference generally predicted for the singlet and triplet states of carbenes, a value of the angle between the carbene bonds, a_{643} , of about 109–115° for the singlet and 125–130° for the triplet.

As already mentioned in the Introduction, for most of the compounds, stable open ketenylcarbenes forms were obtained only at the HF level. The compounds for which the ketenylcarbene structure was maintained at the MP2 level belong to series **a** and **c**, i.e. **I-2a**, **I-3a**, **I-4a**, **I-5a** and **I-4c** and **I-5c**, respectively. These results indicate that the ketenylcarbenes in class **b** might be more susceptible

Table 2. Relevant geometric parameter for the ring closure reaction, a_{432} (°), and the bond order between the carbon atoms, C2 and C4, p_{24}

	a		b		c	
	a_{432}	$p_{24}(\text{HF})$	a_{432}	$p_{24}(\text{HF})$	a_{432}	$p_{24}(\text{HF})$
I-1	108.1	0.088				
I-2	112.83	0.055	104.36	0.208	110.79	0.089
I-3	109.68	0.058	106.49	0.136	107.01	0.083
I-4	113.57	<0.050	— ^a	— ^a	107.57	0.092
I-5	115.21	<0.050	99.63	0.188	111.16	<0.050
I-6	109.78	0.054	107.66	0.070	108.60	<0.050
I-7	108.52	0.084	99.55	0.168	98.96	0.174

^a No stable ketenylcarbene structure could be located.

to undergo cyclization than the other two classes. We can assume that the differences in the electronic structures of classes **a** and **c** on the one hand and class **b** on the other may provide some indications of those features mostly implied in the ring closure reaction. Secondly, the same indications can be obtained by analyzing the changes brought about by introducing the electronic correlation, i.e. MP2 vs HF. A summary of the results indicating the level of calculation, HF/6–31G*//HF/6–31G* (HF) or MP2/6–31G*//MP2/6–31G* (MP2), at which ketenylcarbenes structures were located is indicated in Fig. 1.

The main difference in the HF optimized geometry of ketenylcarbenes in series **a** and **b** consists in the lower values of the bond angle a_{432} for the latter class. As for ketenylcarbenes in series **b**, MP2 optimization leads to cyclopropenone structures so we can consider this as a sign of the enhanced propensity of series **b** to undergo the ring closure reaction. The same tendency is also reflected by the bond order values (p_{24}) between the atoms C2 and C4, non-bonded in the ketenyl structures. The data in Table 2 show significant larger values of p_{24} for series **b**.

The ketenylcarbenes **I-5b** and **I-5c** deserve special mention. The geometry at the minimum energy point corresponds to a pyramidal structure of the NH_2 group substituted on C3, i.e. close to the ketenyl fragment. The planar structure is higher in energy with 14.20 kcal mol^{−1}. This structure is similar to that of the amine group in ketenamine and is not influenced by the carbene moiety.

Ring closure reaction of ketenylcarbenes. According to the experimental data, the ring closure reaction represents the main reaction of the ketenylcarbene intermediates. The calculation of the activation energies leads to values in the range 2–12 kcal mol^{−1} for class **a** and lower values, similar to those previously reported, for class **c**. In all cases, the main feature of the TS geometry in comparison with the equilibrium geometry is the decrease of the bond angle, a_{432} , reflecting the formation of the three-membered ring. The C3–C4 bond length approaches the value of a double bond. For the ketenylcarbenes **I-2a**, **I-4a** and **I-5a**, characterized by larger

Table 1. Hartree–Fock-calculated singlet–triplet gap, ΔE_{ST} (kcal mol^{−1}), for the ketenylcarbenes

	a	b	c
I-1	2.18	2.18	2.18
I-2	19.91	11.95	23.60
I-3	11.66	7.92	15.49
I-4	28.68	— ^a	33.24
I-5	28.52	6.48	42.43

^a No stable singlet ketenylcarbene structure was located.

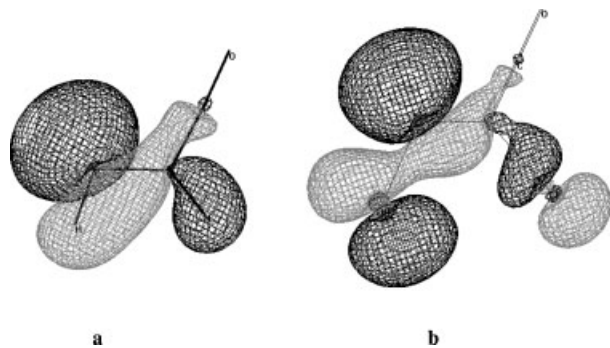


Figure 2. Highest occupied molecular orbital (*homo*) of *syn*-ketenylcarbenes: (a) **I-1**; (b) **I-3a**

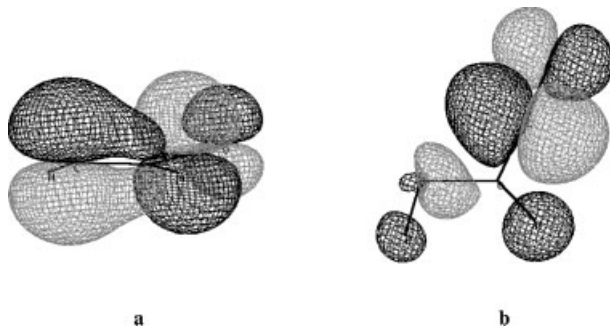


Figure 3. First two vacant molecular orbitals of the ketenylcarbene **I-1**: (a) *lumo1*; (b) *lumo2*

values of the activation energies, 10–12 kcal mol^{−1}, the transition states could also be located at the MP2 level. At this level we found a significant decrease of the activation energy, down to around 2–3 kcal mol^{−1}. The larger values for the bond angle α_{432} reflect an earlier transition state than for HF calculations.

Two aspects, generally considered in connection with the electrocyclic reactions, will be discussed in the following: the nucleophilic attack of the carbene lone pair on the vacant orbital localized on the C α of the ketenyl fragment and the role of the electrostatic interactions between the atoms implied in the ring closure reaction. Some relevant theoretical data regarding the features of the frontier molecular orbitals and the charge distribution are presented in Figs 2 and 3 and in Tables 3–5.

The highest occupied molecular orbital, *homo*, is a σ -orbital localized in the molecular plane; it corresponds mainly to the carbene lone pair [Fig. 2(a)]. The degree of

Table 4. The atomic population on C4 in the highest occupied molecular orbital, $n(4)$, the *homo*–*lumo* gap, $\Delta\epsilon$ (ha), and the product of charge densities of the atoms implied in the ring closure reaction, q_2q_4 , calculated at the HF/6–31G*//HF/6–31G* level for ketenylcarbenes in class **b**

	I-2b	I-3b	I-5b	I-6b	I-7b
$n(4)$	1.642	1.614	1.655	1.693	1.646
$\Delta\epsilon$ (ha)	0.4801	0.4629	0.4861	0.4754	0.4881
q_2q_4	−0.186	−0.162	−0.168	−0.1491	−0.170

localization on C4 is well reflected by the calculated Mulliken atomic population in the highest occupied molecular orbital, $n(4)$: a value close to 2 indicates a higher degree of localization on the carbene center.

The data in Table 3 show that the values of $n(4)$ are around 1.60–1.72, except for the chlorine and cyan C4-substituted ketenylcarbenes, **I-3a**, **I-3c** and **I-6a**. For these ketenylcarbenes, $n(4)$ is lower, ~ 1.3 , reflecting the conjugation of the lone pair of the substituent with the carbene lone pair, as can be seen for **I-3a** in Fig. 2(b).

The first vacant orbital, hereafter labeled as *lumo1* is a π -orbital, orthogonal to the molecular plane, and has a high degree of localization on both the carbene and the ketene C α carbons. The next vacant orbital, *lumo2*, is the characteristic vacant orbital of the ketenes. It is localized in the molecular plane and corresponds to the in-plane π antibonding interaction of the π -orbitals of O and C. A typical example for the HF vacant orbitals is given in Fig. 3 for **I-1**.

Some inversions in this general sequence of the frontier orbitals were observed at both HF and MP2 levels. Thus, for **I-4a** at the HF level and for **I-5a** at both levels, *lumo1* represents the in-plane vacant orbital localized on the ketenyl fragment. The sequence of the first two vacant orbitals was found to be also dependent on the basis set, i.e. for dichloroketenylcarbene at the STO 3–21G level *lumo1* is localized on the ketene and *lumo2* on the carbene center.

At the MP2 level, all three frontier orbitals were stabilized; the effect was larger for the vacant orbital located in the molecular plane, resulting in a decrease in the corresponding energy gap, $\Delta\epsilon$.

Considering the features of the vacant molecular orbitals, we can assume that the ketenyl carbon C α represents a possible center for two nucleophilic attacks:

Table 3. The atomic population on C4 in the highest occupied molecular orbital, $n(4)$, the *homo*–*lumo* gap, $\Delta\epsilon$ (ha), and the product of charge densities of the atoms implied in the ring closure reaction, q_2q_4 , calculated at the HF/6–31G*//HF/6–31G* and MP2/6–31G*//MP2/6–31G* levels for ketenylcarbenes in class **a**

	I-1 HF	I-2a		I-3a		I-4a		I-5a		I-6a HF	I-7a HF
		HF	MP2	HF	MP2	HF	MP2	HF	MP2		
$n(4)$	1.720	1.622	1.614	1.285	1.259	1.604	1.595	1.678	1.671	1.358	1.617
$\Delta\epsilon$ (ha)	0.4777	0.4904	0.4883	0.4601	0.4585	0.4870	0.4840	0.4853	0.4804	0.4724	0.4804
q_2q_4	−0.157	0.197	0.094	−0.061	−0.092	0.118	0.036	0.102	0.035	0.038	−0.011

Table 5. The atomic population on C4 in the highest occupied molecular orbital, $n(4)$, the *homo*–*lumo* gap, $\Delta\epsilon$ (ha), and the product of charge densities of the atoms implied in the ring closure reaction, q_2q_4 , calculated at the HF/6–31G*//HF/6–31G* and MP2/6–31G*//MP2/6–31G* levels for ketenylcarbenes in class **c**

	I-1 HF	I-2c HF	I-3c HF	I-4c		I-5c	
				HF	MP2	HF	MP2
$n(4)$	1.720	1.618	1.294	1.603	1.574	1.677	1.603
$\Delta\epsilon$ (ha)	0.4777	0.4785	0.4420	0.4707	0.4831	0.4772	0.4713
q_2q_4	–0.157	0.154	–0.076	0.087	0.025	0.088	0.022

an out-of-plane attack on the π vacant orbital, generally *lumo1*, by an electron pair orthogonal to the molecular plane and an in-plane attack on the other vacant orbital, *lumo2*, by a lone pair localized in the molecular plane.

The localization of the carbene lone pair in the plane of the molecule implies that the ring closure reaction leading to cyclopropanone might be due to the in-plane attack and therefore will be determined by the *homo*–*lumo2* interaction for **I-2a** and **I-3a** at both HF and MP2 levels and for **I-4a** at the HF level and by the *homo*–*lumo1* interaction for **I-4a** (MP2) and **I-5a** (HF, MP2). Under this assumption, the reactivity of the ketenylcarbenes will be dependent on two factors, the degree of localization of the highest occupied molecular orbital on the carbene center and the gap $\Delta\epsilon$ between the frontier orbitals implied in the *homo*–*lumo1* or *homo*–*lumo2* interaction, depending on the carbene.

The $\Delta\epsilon$ values in Tables 3–5 allow the following observations. Considering the *homo*–*lumo* gap, the fluoroketenylcarbene **I-2a** occupies a special position, presenting the largest value; it is followed by **I-4a** and **I-5a**, that is, by the carbenes for which open ketenylcarbene structures were found even at the MP2 level. The ketenylcarbenes for which at the HF level $\Delta\epsilon$ has lower values are more susceptible to undergo cyclization on attempted MP2 optimization. This is the case for **I-1**, **I-3a** and **I-6a**. However, for **I-3a** an equilibrium geometry corresponding to the open, uncyclized form was located at the MP2 level. This could be explained by the factor opposing the nucleophilic attack leading to cyclization, that is, the degree of localization of the *homo* on the carbene center; we have seen that the chlorine substitution determines the lowest value of $n(4)$.

In order to check if the nucleophilic attack could be considered as a driving force for the ring closure reaction, we calculated the potential energy surface of the ketenylcarbenes in terms of the torsion about the C4–C3 bond, the dihedral d_{6435} . At a certain value, this torsion will bring the in-plane carbene lone-pair in a position susceptible to attack the orthogonal vacant π -orbital, *lumo1*. If the nucleophilic attack is the driving force for ring closure, it is expected that optimization will lead to cyclopropanones.

The dihedral was varied with a step of 10° , all the other internal coordinates being fully optimized. It was found that for values around 65 – 85° some ketenylcarbenes

undergo a spontaneous cyclization process on attempted geometry optimization. These are **I-1**, **I-7a**, all the carbenes in class **b** and **I-3c**. A typical example, the potential energy surface (PES) for **I-1**, is presented in Fig. 4.

It can be seen that the energy increases monotonically toward the value corresponding to the transition state for the *syn*–*anti* isomerization process, up to the values of 70 and 80° . For these values there is a break in the plot and the energy is close to the value for cyclopropanones. The angle a_{432} reaches a value of about 62° , characteristic of the cyclopropanone ring. For larger values of d_{6435} the plot again takes the expected aspect.

The results for series **b** are not very conclusive. On the one hand, the geometric parameter, a_{432} , the bond order between C2 and C4 and the results of optimizations at the MP2 level which predict cyclopropanones structures point to the fact that this class will be more predisposed to cyclize. On the other hand, the $\Delta\epsilon$ values are similar to those of the compounds in series **a**, for which ketenylcarbene structures were obtained at the MP2 level. We presume, therefore, that there is also another factor that is implied in the high reactivity of this class.

Considering series **c**, we can assume that for the ketenylcarbenes with a value of $n(4)$ around 1.6 – 1.7 , a

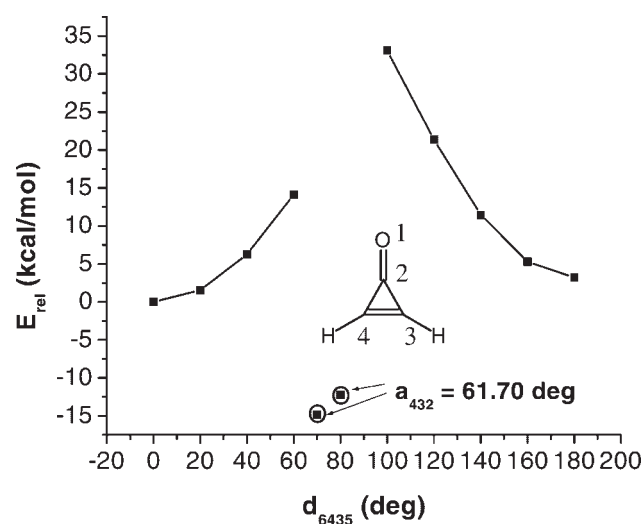


Figure 4. The potential energy surface for the ketenylcarbene **I-1** with respect to the torsion around the C3–C4 bond

$\Delta\epsilon$ value of about 0.470–0.478 ha is the limit for preventing cyclization at the HF level; as the effect of MP2 calculations is to decrease the $\Delta\epsilon$ value, we can understand why at this level the cyclization process is favored.

Taking in to account the results for class **b**, we have also considered another aspect inferred in discussing the electrocyclic reactions, i.e. the electrostatic interaction.¹² In our case the most important atoms are C2 and C4 directly implied in the ring closure. An estimation of the electrostatic interaction energy, E_{el} (kcal mol⁻¹), was made considering the formula $330.7q_2q_4/r_{24}$ (Å), where q_2 and q_4 represent the Mulliken atomic charges and r_{24} is the distance between C2 and C4. As this distance can be considered to be very similar in all the compounds, the electrostatic repulsive or attractive interaction between both atoms is in fact determined by the product q_2q_4 . Considering the Mulliken charges on these atoms, the following observations can be made.

The charge on C2, q_2 , has an almost constant positive value in the range 0.60–0.68, reflecting the known electronic feature of the ketene C α atom, whereas q_4 is significantly influenced by the substituent. For class **a**, at the HF level, the interaction is strongly attractive for **I-1**, the charge distribution representing a positive factor for the tendency to cyclization. Although attractive interactions are also predicted for **I-3a** and **I-7a**, the low q_2q_4 values indicate that the electrostatic contribution will not be an essential factor in the reactivity of these ketenylcarbenes. For **I-2a**, **I-4a** and **I-5a**, the predicted repulsive interaction prevents the ring closure.

At the MP2 level, the charges on both C2 and C4 are decreased in comparison with the HF values. These changes in the charges of both atoms determine either a decrease in the repulsive interaction which had prevented the cyclization at the HF level (**I-2a**, **I-4a** and **I-5a**) or an increase in the electrostatic attraction (**I-3a**). The overall effect is an enhanced probability for the ring closure reaction.

In order to obtain better evidence for the role of electrostatic interaction in the ring closure reaction, the activation energy for the ketenylcarbenes in class **a** was plotted against the electrostatic energy (Fig. 5). The plot reflects a quasi-linear dependence as long as the methyl-containing ketenylcarbene is not included.

In the case of carbenes in class **b**, the charges on C2 do not change to a great extent whereas the charges q_4 became all negative, resulting a significantly increased electrostatic attraction. As we have already seen that the optimization at the MP2 level has as the main effect either a decrease of the C2, C4 repulsion or an increase of the attraction between the same atoms, it is predictable that at the MP2 level all these ketenylcarbenes will cyclize.

The results obtained for series **c** predict a lower repulsion (**I-2c**, **I-4c**, **I-5c**) or an enhanced attraction (**I-3c**) with respect to series **a**. The bond order between C2 and C4 is in the range 0.080–0.092 for all the compounds except **I-7c**, for which it is larger, 0.174.

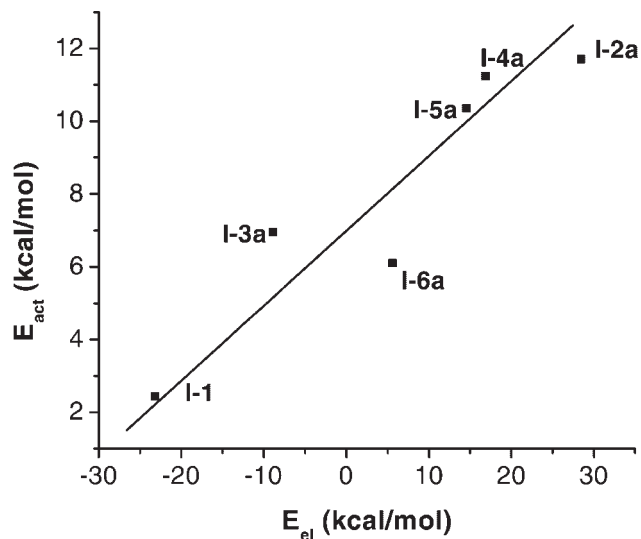


Figure 5. Plot of the activation energy of the ring closure reaction against the electrostatic interaction of C2 and C4

One expects a lower tendency for the ring closure reaction compared with series **b**, but large enough to prevent location of stable carbene geometries at the MP2 level.

Ring opening reaction of cyclopropanones. One of the pathways leading to the alkynes could be the ring opening of the cyclopropanones followed by CO elimination. The located transition states for this reaction are the same as those for the ring closure reaction. The corresponding activation energies are given in Table 6. The trend in the activation energies for the ring opening reaction of cyclopropanones is **a** < **c** < **b**.

CO elimination reaction ($TS_{CO\ elim}$). The activation energies for the CO elimination from the *syn*-ketenylcarbenes are given in Table 7.

The main reaction coordinate is the distance r_{23} between the atoms C2 and C3. The transition states are

Table 6. Activation energies (kcal mol⁻¹) for the ring opening reaction of cyclopropanones

II-1	II-2			II-3		
	a	b	c	a	b	c
26.34	17.66	26.61	20.16	18.93	26.23	20.05

Table 7. Activation energy (kcal mol⁻¹) for the CO reaction of elimination reaction of ketenylcarbenes

I-1	I-2			I-3		
	a	b	c	a	b	c
22.98	50.71	19.96	44.80	37.56	25.20	22.48

characterized by r_{23} values in the range 1.7–1.9 Å and by a strong decrease in r_{34} in comparison with the value in the starting compounds, reflecting the early formation of the triple bond. The linear structure of the ketenyl fragment is lost, for all the compounds the CO elimination occurring under an angle α_{321} in the range 155–158°. A comparison between the monosubstituted ketenylcarbenes in classes **a** and **b** shows lower predicted activation energies for carbenes **b**; for these carbenes, the C2—C3 bond lengths are the lowest, suggesting an earlier transition state. In the case of the fluoro-substituted carbene **I-2b**, the lower value of the activation energy for the decarbonylation reaction can be explained by the destabilizing effect exerted by fluorine on ketenes.¹³

At the MP2 level, the location of the transition state for the CO elimination was possible only for **I-1**, **I-2a** and **I-3a**. The main difference compared with the HF-optimized $\text{TS}_{\text{CO elim}}$ consists in lower values for the C2—C3 bond length, i.e. 1.56–1.65 instead of 1.70–1.85 Å.

For the carbenes **I-2b**, **I-3b** and **I-3c**, during the search for the transition state an *anti* conformation was found with low activation energies. As the *syn-anti* isomerisation requires higher energies (~ 25 – 30 kcal mol^{-1}), this transition state might reflect an inversion reaction at the carbene center.

Excited-state reactivity

For those compounds for which experimental data were available, the unsubstituted and the fluoro- and chloro-substituted *syn*-ketenylcarbenes, and also for the corresponding cyclopropenones, the ground- and excited-state geometries were optimized under the same conditions using the non-gradient optimization method, the only method available for the excited states.

The relative energies of the main stationary points localized on the ground- and excited-state potential energy surfaces are summarized in Table 8. For all the compounds the lowest points on the potential energy surfaces, the ground-state energies of cyclopropenones were taken as

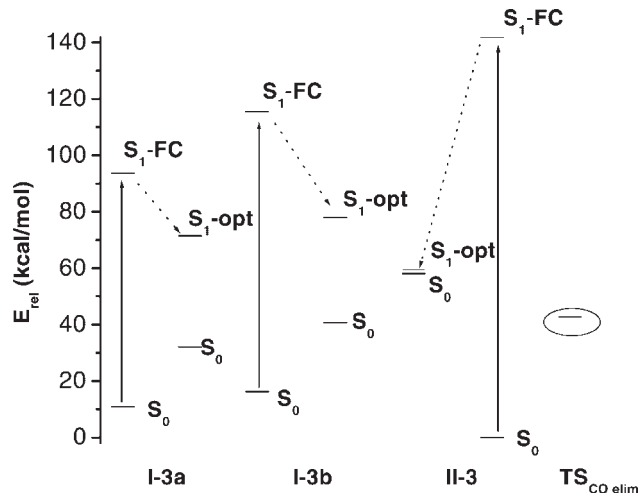


Figure 6. Relative energies of the ground and excited states of chloroketenylcarbenes **I-3a** and **I-3b**, monochlorocyclopropenone **II-3** and the transition states, $\text{TS}_{\text{CO elim}}$, starting from the two ketenylcarbenes

zero energy. FC represents the Frank–Condon transitions, leading to the vertical excited states S_1 , and opt stands for the energy of the optimized excited-state geometries. The CIS energies calculated at the geometry of the S_0 transition state for the CO elimination were also included. A typical example of the relative energies of the ground and excited states is given in Fig. 6 for the monochloro-substituted compounds, **I-3a**, **I-3b** and **II-3a**.

Excited-state structures of ketenylcarbenes (I).

The energies of the ground state of the ketenylcarbenes calculated using the non-gradient technique correspond to those found using the normal gradient optimization techniques with CI calculations.

The geometries are also similar to those calculated previously, except for class **b** of ketenylcarbenes for which the angle α_{432} was found to be smaller than that obtained by the former optimization. As this is the critical parameter for the stability of the ketenylcarbenes in the open form and the most sensitive to the method used, it

Table 8. Significant points on the ground- and excited-state potential energy surfaces of ketenylcarbenes (I) and cyclopropenones (II)

	1	2a	2b	2c	3a	3b	3c
$S_0(\text{II-opt})^a$	0.00	0.00	0.00	0.00	0.00	0.00	0.00
$S_1(\text{II-FC})^b$	136.45	156.38	156.38	172.66	141.66	141.66	149.62
$S_0(\text{II-FC})$	49.68	49.36	42.36	56.08	59.09	40.96	38.38
$S_1(\text{II-opt})$	69.82	52.96	77.64	73.28	59.38	78.00	85.04
$S_0(\text{I-opt})$	22.81	7.04	10.90	17.32	10.84	16.23	16.30
$S_1(\text{I-FC})$	100.53	100.09	118.37	112.46	93.05	116.31	108.06
$S_0(\text{I-FC})$	47.51	21.65	38.38	37.84	32.11	40.70	38.29
$S_1(\text{I-opt})$	72.51	75.27	91.34	79.99	71.44	78.00	85.04
$\text{TS}_{\text{cyc}} + \text{CI}$	45.21	37.53	46.48	43.00	29.57	36.87	27.91
$\text{TS}_{\text{CO}} + \text{CI}$	41.92	48.35	39.10	49.55	41.71	42.77	49.07

^a opt represents the energy of the totally optimized geometry.

^b FC represents the energy of the FC state at the corresponding totally optimized geometry.

can be said that the non-gradient optimization predicts an enhanced propensity towards cyclization.

In the excited states, the changes in the geometries are similar for all the carbenes, being slightly influenced by the type of substituent. The only different behavior was noted for **I-2b**. Starting as for all the other ketenylcarbenes with the *syn* conformer, during the optimization of the excited state the *anti* conformer was obtained. The same change in the conformation was observed in the ground-state MP2 search of the transition state for the CO elimination. This fact was assigned to an inversion at the carbene center. The optimized S₁ geometry maintains the linear structure of the ketenyl fragment. This is different from the excited-state geometry of the mono- and di substituted fluoro- and chloroketenes for which the calculations predict bent excited-state structures.

In the following, the main modifications in the excited state will be discussed in relation to the two considered reactions.

The main coordinate describing the transition state for the ring closure reaction is the angle a_{432} . It has already been discussed that the lower the value of this angle, the larger is the probability of ring closure. The calculations for the ketenylcarbenes' first excited state predict larger a_{432} values than in the ground state, i.e. values around 122.5–124.5° in comparison with those found in S₀, 90–112° (Table 9). We can therefore assume that in the excited state, the probability of the ring closure reaction is diminished. The values for a_{432} in the ground state listed in Table 9 are different from those given in Table 2 obtained during the normal gradient optimization.

Considering the CO elimination reaction, in all cases the energy of the transition state, TS_{CO elim}, was found at lower values than that of the carbene S₁ state. However, although an increase in the C2—C3 distance (r_{23}) together with a decrease in r_{34} is noted, the values are far enough from those in the transition state, TS_{CO elim}.

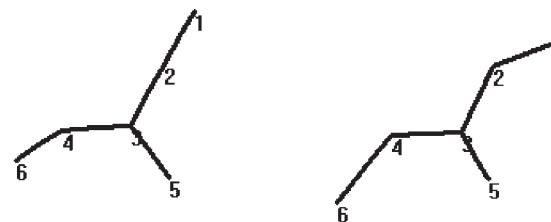
The optimized excited states of the ketenylcarbenes are lower than the FC states by about 21–38 kcal mol^{−1}, the smallest relaxation energy from the FC state being obtained for **I-3a**, 21.61 kcal mol^{−1} (Fig. 6). At the optimized geometry of S₁, the S₁–S₀ energy gap is strongly diminished in comparison with the FC value starting from the S₀ minimum. The values ranges from 25 kcal mol^{−1} (**I-1**) to ~54 kcal mol^{−1} (**I-2a** and **I-2b**).

Excited-state geometry of cyclopropenones (II).

The calculations show that for all cyclopropenones in the excited state, the cyclopropane ring is opened, the

Table 9. The value of the bond angle a_{432} (°) in the optimized ground and excited states of the ketenylcarbenes (non-gradient optimizations)

	I-1	I-2a	I-2b	I-2c	I-3a	I-3b	I-3c
S ₀	98.74	112.23	85.2	103.15	110.97	89.31	102.34
S ₁	123.48	124.09	124.60	124.51	124.24	123.49	122.45



	II-1	II-2b	II-3b	II-3c	II-2a	II-2c	II-3a
r_{23}	1.342	1.369	1.357	1.347	1.422	1.417	1.443
r_{34}	1.363	1.353	1.363	1.379	1.378	1.367	1.356
a_{321}	180.0	180.0	179.9	180.0	136.4	133.8	135.8
a_{432}	123.8	121.3	123.8	122.5	119.4	126.0	115.4
a_{534}	125.9	124.3	121.4	122.2	119.2	117.9	123.7
a_{643}	150.9	151.2	145.1	142.4	125.6	121.8	130.1

Figure 7. Geometry of the optimized excited singlet state of cyclopropenones

resulting geometry reflecting a ketenylcarbene structure. In the case of monosubstituted fluoro- and chlorocyclopropenones, the ring opening can occur in two ways, leading to ketenylcarbenes in series **a** and **b**, respectively. As can be seen in Table 8, the lowest energy corresponds to the formation of ketenylcarbenes belonging to series **a**. The comparison of the optimized S₁ results for all the cyclopropenones reveals two kinds of geometry, labeled A and B in Fig. 7. For the cyclopropenones **II-1**, **II-2b**, **II-3b** and **II-3c** (Fig. 7, A) a ketenylcarbene-like structure was obtained, the ketenyl fragment retaining its usual linear shape. The similarity with the S₁ geometry of the related ketenylcarbenes is almost perfect for **II-1**, **II-3b** and **II-3c**. The energy difference between both optimized excited states is very small, 2.69 kcal mol^{−1} for **II-1** and practically zero for **II-3b** and **II-3c**. A large energy difference was obtained between the optimized S₁ states of **II-2b** and **I-2b** and is due to the different conformer predicted by the calculations. The optimization of the cyclopropenone led to the *syn* conformer whereas, as has already been discussed, for the excited state of the corresponding ketenylcarbene the *anti* conformation was obtained.

The S₁ ring opening of the other cyclopropenones, **II-2a**, **II-2c** and **II-3a** (Fig. 7, B) leads to a distorted ketenyl structure characterized by a bent form of the ketene fragment. At the same time the C2—C3 distance is larger than for the ketenylcarbenes. The trend of the variation of both these parameters reflects a tendency towards CO elimination.

CONCLUSIONS

The comparison of the theoretical predictions with the available experimental data leads to the following observations. As long as the ketenylcarbenes are formed, the cyclization to cyclopropenones is the most likely process. In agreement with the experimental data, the calculations predict a lower propensity for this reaction for the fluoroketenylcarbene. A similar reactivity is also

predicted for the amino- and hydroxy-substituted carbenes. The lack of experimental data at present prevents testing of this result.

The theoretical results support the assumption that, especially in cases **b** and **c**, the electrostatic interaction between the atoms directly implied in the new bond formation represents the main factor in the reactivity towards the ring closure reaction.

Under continuous irradiation, the cyclopropenones first reach their FC excited state and relax quickly to their optimized geometry. The optimized S_1 energies are significantly decreased, reflecting the drastic geometric change that occurs upon excitation. The maximum differences between the FC and the optimized energies of the S_1 state were found for the fluorine-containing cyclopropenones, **II-2a**, **II-2c**, and for the monochlorocyclopropenone **II-3a** and are in the range 103.4–82.3 kcal mol⁻¹.

The monosubstituted derivatives **II-2a** and **II-3a** deserve a special mention. At the geometry of S_1 , the S_1 – S_0 gap is very small, allowing for the possibility of a state crossing. The open shape predicted for these states shows that from this point the reaction will evolve in a different direction than cyclization and one of the most probable routes is decarbonylation.

Supplementary material

Additional material is available in Wiley Interscience.

Acknowledgment

Financial support from CNCSIS-Romania, grant 33618/2002, is gratefully acknowledged.

REFERENCES

1. Monnier M, Allouche A, Verlaque P, Aycard JP. *J. Phys. Chem.* 1995; **99**: 5977–5985.
2. Pietri N, Monnier M, Aycard JP. *J. Org. Chem.* 1998; **63**: 2462–2468.
3. Aycard JP, Allouche A, Cossu M, Hillebrand M. *J. Phys. Chem.* 1999; **103**: 9013–9021.
4. Mincu I, Hillebrand M, Verlaque P, Allouche A, Cossu M, Aycard JP, Pourcin J. *J. Phys. Chem.* 1996; **100**: 16045–16052.
5. Ionescu A, Pietri N, Hillebrand M, Monnier M, Aycard JP. *Can. J. Chem.* 2002; **80**: 455–461.
6. Ionescu A, Pietri N, Hillebrand M, Monnier M, Aycard JP. *Rev. Roum. Chim.* 2002; **47**: 71–79.
7. Allen AD, Colomvakos JD, Diedrich F, Egle I, Hao X, Liu R, Luszyk J, Ma J, McAllister MA, Rubin Y, Sung K, Tidwell TT, Wagner BD. *J. Am. Chem. Soc.* 1997; **119**: 12125–12130.
8. Brahm JC, Dailey WP. *J. Am. Chem. Soc.* 1989; **111**: 8940–8941.
9. Dailey WP. *J. Org. Chem.* 1995; **60**: 6737–6743.
10. Sung K, Fang D-C, Glenn D, Tidwell TT. *J. Chem. Soc., Perkin Trans. 2* 1998; 2073–2080.
11. Schmidt MW, Baldridge KK, Boatz JA, Elbert ST, Gordon MS, Jensen JJ, Koseki S, Matsunaga N, Nguyen KA, Su S, Windus TL, Dupuis M, Montgomery JA. *J. Comput. Chem.* 1993; **14**: 1347–1363.
12. Scuseria GE, Duran M, Maclagan RGAR, Schaefer HF. *J. Am. Chem. Soc.* 1989; **111**: 3071–3076.
13. Jiao H, Schleyer PvR. *J. Am. Chem. Soc.* 1995; **117**: 11529–11535.